



# Glycation increases human annulus fibrosus stiffness in both experimental measurements and theoretical predictions

Diane R. Wagner<sup>a</sup>, Karen M. Reiser<sup>b</sup>, Jeffrey C. Lotz<sup>a,\*</sup>

<sup>a</sup>*Orthopaedic Bioengineering Laboratory, Department of Orthopaedic Surgery, University of California, San Francisco, CA, USA*

<sup>b</sup>*Department of Neurosurgery, University of California at Davis, CA, USA*

Accepted 18 February 2005

---

## Abstract

One of the primary age-related changes to collagenous tissues is the increased concentration of advanced glycation endproducts (AGEs). Although AGEs have been shown to increase the mechanical stiffness of many tissues, their influence on the mechanical properties of the annulus fibrosus has not been measured experimentally. In previous theoretical work, we hypothesized that the mechanical influence of AGEs on the annulus could be represented in an additive strain energy function with a separate crosslinking term, but the material coefficients associated with this term were not correlated with AGE concentration. In the current study, we measured the tensile stress–strain response of the human annulus in the axial direction both before and after glycation with methylglyoxal. Using nonlinear regression, the strain energy function was simultaneously applied to these new data and to data from a wide range of experimental protocols reported in the literature to determine values for the material coefficients appearing in the constitutive equation. Nonenzymatic collagen crosslinking induced a statistically significant change in annular material properties. Furthermore, the concentration of AGEs correlated positively with the material coefficients found in the terms of the strain energy function that we associate with collagen crosslinking. These data suggest that AGEs contribute to age-related disc stiffening as well as validate the hypothesis that biochemical constituents can be related mathematically to tissue behavior. In the future, this structurally guided constitutive relationship may provide further insight into the structure–function relationships of the annulus fibrosus.

© 2005 Elsevier Ltd. All rights reserved.

*Keywords:* Nonenzymatic glycation; Annulus fibrosus; Strain energy; Mechanical properties; Collagen crosslinking

---

## 1. Introduction

The complex biomechanical function of the annulus fibrosus is facilitated by a composite architecture composed of collagen fibers arranged in a series of concentric layers called “lamellae”. Within a single lamella, the collagen fibers are parallel and are oriented approximately  $\pm 60^\circ$  from the vertical axis of the body at the periphery of the disc; this angle decreases linearly to  $\pm 45^\circ$  in the inner annulus (Cassidy et al., 1989; Hukins, 1988; Marchand and Ahmed, 1990). The fibers

in adjacent lamellae run in opposite directions, forming a structure that is similar to an angle-ply composite. The fibrillar collagen in the lamellae is imbedded in a ground substance composed primarily of proteoglycans.

The human annulus fibrosus exhibits an increased modulus in confined compression and a decreased tensile strength with age-related degeneration (Acaroglu et al., 1995; Fujita et al., 1997; Iatridis et al., 1998). Although the molecular basis for these changes is unknown, progressive glyco-oxidative damage to the matrix, as measured by the accumulation of advanced glycation end-products (AGEs), has been implicated in the commonly observed degeneration and impaired material function of the aging intervertebral disc (Hormel and Eyre, 1991). In other collagenous tissues

---

\*Corresponding author. Tel.: +1 415 476 7881;  
fax: +1 415 476 1128.

E-mail address: [jlotz@itsa.ucsf.edu](mailto:jlotz@itsa.ucsf.edu) (J.C. Lotz).

such as skin, cartilage, and artery (Chen et al., 2002; Reihnsner and Menzel, 1998; Verzijl et al., 2002; Wolffenbittel et al., 1998), increased levels of AGEs have been shown to increase tissue stiffness, but the effect of AGE accumulation on the mechanical properties of the annulus fibrosus has not been previously studied.

AGEs comprise a diverse group of compounds that arise from any of several pathways, including the nonenzymatic glycation of lysine residues and oxidation of fatty acids. AGEs accumulate over time in long-lived proteins such as collagen (Reiser, 1998). Most AGEs have intrinsic fluorescence and can be quantified by measuring tissue fluorescence at the appropriate excitation and emission wavelengths. Several AGEs have been structurally and functionally characterized (Thorpe and Baynes, 2003); tissue levels of these specific compounds, such as pentosidine (Sell and Monnier, 1989) are correlated with tissue levels of AGEs.

We hypothesize that the macromolecular structure of the annulus, including the quantity and distribution of AGE crosslinks, determines the tissue's mechanical properties. Our long-term goal is to develop a mathematical model that links annular tissue architecture to material properties and that clarifies structure–function relationships in the intervertebral disc. We have previously described an annular strain energy function with separate terms representing specific tissue features such as the matrix, the fibers, and the interactions between constituents (Wagner and Lotz, 2004). One advantage of this formulation is that macromolecular constituents are associated with particular terms of the strain energy function. This allows for the possibility that biochemical measures can be correlated with particular material parameters, and in doing so, provide insight into mechanisms of tissue degeneration. For example, the interactions term of this previous strain energy function was designed specifically to model collagen crosslinks within an annular lamella. However, it was not previously determined whether the coefficients of the interactions term correlate with the concentration of AGEs.

The first objective of this study was to better understand the effects of AGEs on the annular tensile stiffness. To do so, we subjected annular tissue specimens to mechanical tests both before and after they had been incubated with methylglyoxal, a methylated oxaldehyde intermediate found in vivo that rapidly induces formation of AGEs in vitro (Anderson et al., 1994; Reiser, 1998). The second objective was to validate that the interactions terms of the annular strain energy function accurately represent the mechanical effects of collagen crosslinks. We modified our previously proposed strain energy function by adding an additional term and demonstrated that the mechanical changes due to increased concentration of AGEs can be modeled by

increasing particular material coefficients that are associated with interactions between the constituents.

## 2. Methods

Human lumbar spines were harvested at autopsy from 7 individuals aged 16–49 years and stored frozen ( $-20^{\circ}\text{C}$ ) until dissection. Tools consisting of two parallel microtome blades fixed at a set distance apart were used to produce rectangular specimens that were 2 mm thick, 5 mm wide, and approximately 10 mm long from the anteriorlateral portion of the L4/5, L3/4, and L2/3 discs, with the longest dimension coinciding with the axial direction (Fig. 1). Ten test specimens were taken from 10 grade I and II (nondegenerate) discs (Thompson et al., 1990). From four of the discs, a second test specimen was taken from the contralateral side and was used as a control (age range 27–49). Both test and control specimens were subjected to mechanical testing, however the control specimens were not matched to their corresponding test specimen in the subsequent analysis. Tissue that was directly adjacent to the test and control specimens in the intact disc was returned separately to the freezer for later biochemical analysis.

In order to minimize swelling of the tissue during testing, the specimens were soaked overnight in a 0.15 M saline and protease inhibitors solution consisting of 1 mM EDTA (DS), 1 mM EDTA (TS), 5 mM benzamidine, 10 mM NEM and 1 mM PMSF. On the day of testing, four loops of a continuous piece of undyed, braided polyglactin 910 suture size 4-0 (1.5 metric) (Ethicon, Piscataway, NJ) were sewn with a 24 mm curved needle and were knotted into the ends of the

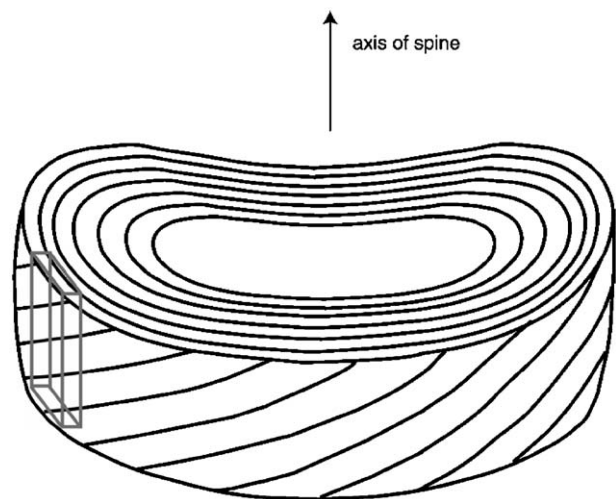


Fig. 1. A test specimen was harvested from the anterior–lateral region of the non-degenerate intact human intervertebral disc, with the longest dimension coinciding with the axial direction.

specimen (Fig. 2). The integrity of the knots was ensured with a drop of fast-drying cyanoacrylate glue, and the glue was kept away from the tissue. Nine dots of black tattoo ink (Basic K6, Superior Tattoo, Phoenix AZ) were applied with the tip of a pin in the middle of the specimen in a grid pattern (grid dimension approximately  $2.5 \times 2.5$  mm) and served as visual targets for the strain measurements (Fig. 2).

The specimens were submerged in the physiologic saline and protease inhibitors solution during testing. The custom testing apparatus and software programs that measure tissue stress and strain have been previously described (Wagner and Lotz, 2004). After the force transducer (25 lb Load Cell Model LCCA, Omega Engineering, Stamford, CT) was zeroed without the specimen in place, the tissue was loaded into the testing apparatus. The tissue was preconditioned with 10 cycles of a 0.04 MPa tensile load at a strain rate of approximately  $0.002 \text{ s}^{-1}$ . The specimen was returned to zero applied load and the distances between the ink dots were measured in this reference configuration for use in the calculation of strain. The specimens were then tested in tension to 0.2 MPa at a strain rate of  $0.0001 \text{ s}^{-1}$  with the forces and the strains recorded every 2 s. Pilot studies showed that the preconditioning regime led to repeatable stress–strain results and that the test stress limits were nondamaging. At the end of testing, specimens were removed from the testing apparatus and allowed to equilibrate for 1 h.

We conducted a pilot study to compare glucose-6-phosphate and methylglyoxal, two glycation agents that are both naturally found in vivo. We chose methylglyoxal for this study because the glucose-6-phosphate protocol took 4 to 8 times longer to achieve similar levels of AGE concentration. The glycation protocol consisted of incubating the test specimens at  $37^\circ\text{C}$  in a solution of 200 mmol Tris/HCL, pH 8.8, containing 100 mmol methylglyoxal (Sigma Aldrich, St. Louis, MO). After one week, test specimens were removed from the glycation buffer and rinsed with PBS. More ink was used to darken the strain measurement dots, if necessary, and the above axial tension test protocol was

repeated. Control specimens were incubated at  $37^\circ\text{C}$  in a sham solution consisting of 200 mmol Tris/HCL, pH 8.8, but without methylglyoxal. Control specimens were also removed from the sham buffer after 1 week and the mechanical test was repeated.

As a general description of the data, an exponential curve of the form  $\sigma = (A/B)(e^{B\epsilon} - 1)$  (Fung, 1967; Kenedi et al., 1965) was fit to the experimental stress–strain data with a Levenberg–Marquardt algorithm (Matlab 5.3, The Mathworks, Inc., Natick, MA), where  $A$  (in MPa) is the modulus at the origin, and  $B$  is a dimensionless measure of nonlinearity. The Poisson's ratio for this uniaxial test was determined by plotting the axial strain (the strain in the direction of applied force) versus the circumferential strain (the strain transverse to the applied force) and fitting a straight line that passed through zero to the data; the Poisson's ratio that we reported was the negative of the calculated slope. We used a paired Student's  $t$ -test to determine whether the coefficients  $A$  and  $B$  and the measured Poisson's ratio had changed with the glycation and sham protocols; significance was set at  $p < 0.05$ .

Because we wanted to estimate the mechanical influence of the AGEs only, without the confounding effect of the 1-week incubation that was seen in the control specimens, we adjusted the observed data from the glycated test specimens after incubation. To accomplish this, we first calculated the percentage change in stress due to the sham protocol at a given strain. We then calculated this percent of the stress at the same strain from the mean data of the test specimens before glycation, and added this amount on to the mean data of the glycated test specimens. This was repeated for multiple strains of the test protocol, and a new exponential curve was fit to this adjusted data.

We used pentosidine content (expressed as nanomolar of pentosidien/mol of collagen) and fluorescence (expressed as arbitrary fluorescence units/mol of collagen) to determine the AGE levels of the glycated and sham specimens as well as of the untreated tissue that had been adjacent to the specimens in vivo. The tissue was first hydrolyzed in 6 N HCl for 24 h at  $110^\circ\text{C}$  and dried. The hydrolysates were dissolved in water and were filtered through a  $0.22 \mu\text{m}$  pore-size Ultrafree-MC microcentrifuge filter (Millipore, Bedford, MA). Aliquots from the acid hydrolysis were assayed for pentosidine by reverse phase HPLC using a 25 cm C-18 column (Vydac, Hesperia, CA). The effluent was monitored at excitation/emission wavelengths of 335/385 nm (Reiser, 1994; Sell and Monnier, 1989). The elution time and quantum efficiency of pentosidine were determined using a pentosidine standard, which had been synthesized by us and characterized as described by us previously (Reiser, 1994). Separate aliquots of the acid hydrolysate were assayed for fluorescence at excitation/emission wavelengths of 370/440 nm using

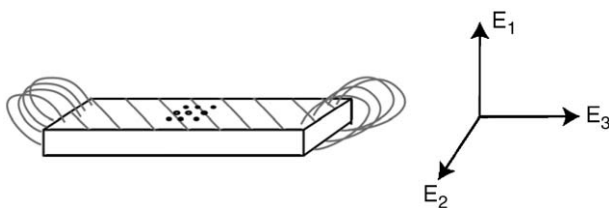


Fig. 2. Four loops of a continuous piece of undyed suture were sewn and knotted into the ends of the specimen. Nine dots of tattoo ink were applied with the tip of a pin in the middle of the specimen in a grid pattern and served as visual targets for the strain measurements. The orthonormal basis  $\mathbf{E}_1$ ,  $\mathbf{E}_2$ , and  $\mathbf{E}_3$  is aligned with the anatomic radial, circumferential, and axial directions, respectively.

an ELISA platereader (Monnier et al., 1984; Reiser, 1994). Collagen content was determined by assaying aliquots of the acid hydrolysates for hydroxyproline using the Woessner colorimetric assay (Woessner, 1961). Unpaired Student's *t*-tests were used to determine whether the tissue's pentosidine content and fluorescence had changed with the glycation and sham protocols.

We have previously described a strain energy function for the annulus consisting of a sum of four separate terms (Wagner and Lotz, 2004). This was accomplished using a composite continuum theory for an isotropic matrix reinforced by two systematically arranged families of fibers that was proposed by Spencer (1984). In this model, the anisotropic properties of the composite are due solely to the fiber families, which are defined by their orientation. We chose a Cartesian basis ( $\mathbf{E}_1$ ,  $\mathbf{E}_2$ ,  $\mathbf{E}_3$ ) to be aligned with the radial, circumferential and axial directions, respectively, of a local anatomic configuration (Fig. 2). The previously proposed strain energy function was

$$W = a_1(I_3 - 1/I_3)^2 + a_2(I_1 I_3^{-1/3} - 3)^2 + \frac{a_3}{b_3}(e^{b_3(I_9-2)} - b_3 I_9) + \frac{a_4}{b_4} e^{b_4(I_{11}-I_9^2+2I_{10})}, \quad (1)$$

where  $I_1$ ,  $I_3$ ,  $I_9$ ,  $I_{10}$ , and  $I_{11}$  are invariant quantities that have been defined by Spencer (1984). In the current study, we modified the previous strain energy function by adding a fifth term:

$$W = a_1(I_3 - 1/I_3)^2 + a_2(I_1 I_3^{-1/3} - 3)^2 + \frac{a_3}{b_3}(e^{b_3(I_9-2)} - b_3 I_9) + \frac{a_4}{b_4} e^{b_4(I_{11}-I_9^2+2I_{10})} + \frac{a_5}{b_5}(e^{b_5(J_9-2)} - b_5 J_9), \quad (2)$$

where  $J_9$  is the sum of the squared stretches in directions perpendicular to the two fiber families. In both the above strain energy functions, the 1st and 2nd terms represent the spherical and deviatoric response of the matrix, respectively. The third term models the collagen fibers with a mechanical response that is stiffer in tension than in compression. The quantity  $I_{11}-I_9^2+2I_{10}$  is equivalent to the sum of the squared shear strains in the two fiber directions, therefore the 4th term represents the resistance of the interactions between constituents (such as collagen crosslinks or fiber-matrix interactions) to shear deformation along the directions of the fibers (Fig. 3a). In Eq. (2) the 5th term represents the resistance of the interactions to stretching in the directions perpendicular to the fibers (Fig. 3b). The coefficients  $a_1$ ,  $a_2$ ,  $a_3$ ,  $a_4$ , and  $a_5$  all have units of MPa, while the coefficients  $b_3$ ,  $b_4$ , and  $b_5$  are dimensionless.

Using previously described methods (Klisch and Lotz, 1999; Wagner and Lotz, 2004), we determined the values of the strain energy coefficients that are specific to the

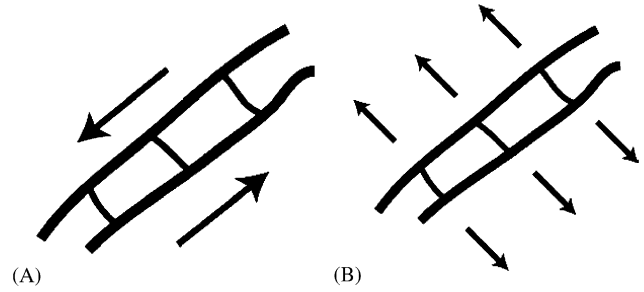


Fig. 3. Interactions terms of the strain energy function represent the resistance of the crosslinks to shear deformation in the direction of the fibers (A) and the resistance of the fibers to stretch deformations in the direction perpendicular to the fibers (B).

annulus for both the above three-dimensional strain energy functions (Eqs. (1) and (2)). To do this, we individually and simultaneously conducted nonlinear regressions to the mean elastic stress-strain response from experimental protocols that span a wide range of annular deformations. The experimental data consisted of: (A) uniaxial tension in the radial direction, non-degenerate anterior middle (Fujita et al., 1997); (B) uniaxial tension in the circumferential direction, non-degenerate anterior middle (Wagner and Lotz, 2004); (C) uniaxial tension in the axial direction, nondegenerate anterior-lateral outer (present study); (D) unconfined compression in the circumferential direction, nondegenerate anterior middle (Wagner and Lotz, 2004); (E) confined compression in the radial direction, nondegenerate lateral middle (Klisch and Lotz, 2000); (F) confined compression in the axial direction, non-degenerate lateral middle (Klisch and Lotz, 2000); (G) biaxial tension, axial stress vs. axial stretch with circumferential stretch held constant at 1.0, nondegenerate anterior outer (Bass et al., 2004); and (H) uniaxial tension in the axial direction, anterior-lateral outer, after incubation in glycation solution (present study). In addition to conducting the simultaneous regressions to the experimental data sets (A)–(H) in the direction of applied stress, we also invoked the stress response for the case of the traction-free surfaces for (A)–(D) and (H), as has been previously described (Wagner and Lotz, 2004). For example, in the radial tension test (A), we also generated the equations for stresses in the circumferential and axial directions. When we conducted the simultaneous regression of the experimental datasets, equations for the traction-free faces were fit to zero stress for the experimental stretches.

The above list of experiments includes two axial tension tests. Experiment (C) measured the stress-stretch properties of the native annular tissue, before it had been incubated in methylglyoxal, and experiment (H) measured the stress-stretch properties of the

annulus after incubation. By including both experiments in the overall nonlinear regressions, we sought to determine whether the interactions terms could adequately describe the influence of AGEs on the tissue's mechanical behavior. Although the form of the stress–strain equations for these two experiments was identical, we allowed the interactions coefficients  $a_4$  and  $a_5$  to take on different values for the two experiments. Specifically, using the first strain energy function, the equations were written such that  $a_4$  was the interactions coefficient for experiments on untreated tissue (A)–(G), while  $a'_4$  was the interactions coefficient only for the equations that described the axial tension experiment using glycated tissue (H). Similarly, in the second strain energy function,  $a_4$  and  $a_5$  were the interactions coefficients for experiments on untreated tissue, while  $a'_4$  and  $a'_5$  were the interactions coefficients only for the axial tension experiment using glycated tissue. In both strain energy functions, other coefficients were allowed to take on only one value for all experiments (A)–(H).

The stress in any one direction depends on all three principal stretches. Therefore, for the experimental protocols (A)–(H) we had to describe the three principal stretches although all were not directly measured. To determine the unmeasured stretches, we made identical assumptions about the Poisson's ratios as in our previous study (Wagner and Lotz, 2004) in all experiments except for  $\nu_{32}$  in experiments (C) and (H). In experiment (C), we used the experimentally measured Poisson's ratio from the untreated tissue of the current study. In experiment (H), we used the experimentally measured Poisson's ratio from the tissue after it had been incubated in methylglyoxal, also from the current study. As in our previous study, the overall statistical fit was extremely sensitive to the Poisson's ratio  $\nu_{23}$  and fiber angle  $\phi$ , therefore we considered  $\nu_{23}$  and  $\phi$  to be parameters best found through the statistical fitting algorithm. We determined best-fit values for the set of coefficients for the first strain energy function  $\{a_1, a_2, a_3, b_3, a_4, b_4, a'_4, \nu_{23}, \phi\}$  using starting values  $\{0.08, 0.005, 0.003, 30, 0.1, 1.0, 0.5, 1.8, 60^\circ\}$  which we chose based on our previous work (Wagner and Lotz, 2004). We determined values of  $\{a_1, a_2, a_3, b_3, a_4, b_4, a_5, b_5, a'_4, a'_5, \nu_{23}, \phi\}$  for the second strain energy function using starting values  $\{0.08, 0.005, 0.003, 30, 0.1, 1.0, 0.001, 5.0, 0.5, 0.1, 1.8, 60^\circ\}$ . We studied the effect of the starting values by considering a wide range. To determine the goodness-of-fit of the solutions, we looked at the sum of the error squared. Finally, we analyzed the covariance matrix, which gives an indication of whether the coefficients are correlated with one another. The values of this matrix range from  $-1$  to  $+1$ , where a value of  $0$  signifies that there is no correlation between the two coefficients, and a value of  $\pm 1$  signifies that the coefficients have a strong positive or negative correlation.

### 3. Results

The exponential equation  $\sigma = (A/B)(e^{B\epsilon} - 1)$  represented the nonlinear tensile axial behavior well, with a correlation coefficient  $>0.95$  for all tests (Fig. 4). The average axial tensile behavior of the test specimens before and after glycation shows a statistically significant increase in the coefficient  $A$  and no statistically significant change in  $B$  with glycation (Table 1) and results in an average stress–strain curve that is slightly stiffer after glycation (Fig. 5). The average tensile behavior of the four control specimens before and after the sham protocol demonstrates a statistically significant decrease in  $A$  and a statistically significant increase in  $B$  (Table 1) and results in an average stress–strain curve that is less stiff after the sham incubation.

Our coefficients of the exponential equation that characterize the average mechanical behavior of the glycated test specimen after adjustment for the softening effect seen in the sham protocol are  $A = 0.178$  and  $B = 10.3$ . By removing the softening effect of the one-week incubation, we note a more pronounced increase in stiffness with glycation (Fig. 5). These data were used as dataset (H) to determine the material coefficients of the strain energy function, as we felt that they best represented the mechanical behavior of the annulus with increased levels of AGEs.

A straight line represented the transverse strain vs. the strain in the direction of applied load reasonably well, with an  $R^2 > 0.80$  for all data. The Poisson's ratio for the test specimens was  $0.89 \pm 0.21$  before glycation and  $0.78 \pm 0.13$  after (Table 1). These results suggest a decreasing trend in the Poisson's ratio of the test specimens with glycation, but are not statistically significant ( $0.1 > p > 0.05$ ). The control specimens, on the other hand, showed no significant change in Poisson's ratio with the sham protocol (Table 1).

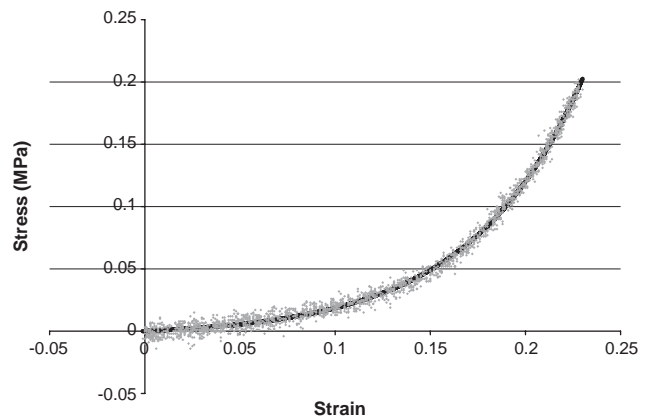


Fig. 4. Representative data from a single specimen shows that the nonlinear tensile axial behavior was well represented by an exponential equation.

Table 1

Average (SD) values for coefficients  $A$  (MPa),  $B$ , and Poisson's ratio  $\nu$ , both before and after glycation or sham treatment. The  $p$  values based on a paired Student's  $t$ -test are also shown

	$A$ (MPa)			$B$			$\nu$		
	Before	After	$p$	Before	After	$p$	Before	After	$p$
Glycation	0.094 (0.048)	0.13 (0.069)	0.032	11.1 (4.7)	10.1 (3.1)	0.18	0.89 (0.21)	0.78 (0.13)	0.068
Sham	0.17 (0.081)	0.075 (0.039)	0.017	6.4 (1.1)	8.1 (1.4)	0.039	1.12 (0.23)	1.11 (0.12)	0.42

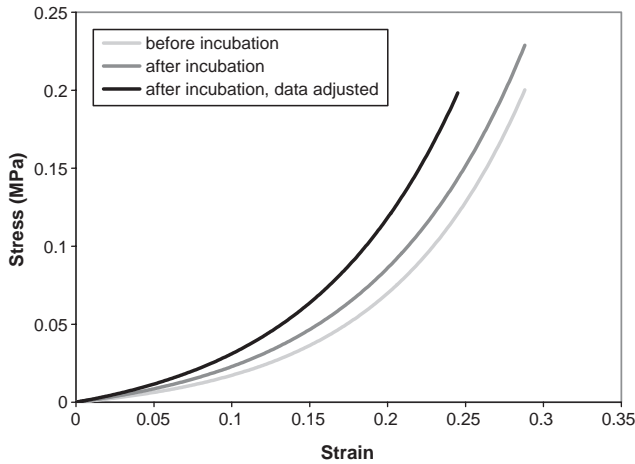


Fig. 5. Test specimens were slightly stiffer in the axial tension test after incubation in a methylglyoxal solution than they were before. We adjusted the data from the test after incubation to eliminate the softening effect of the 1-week incubation. These results show a more pronounced increase in stiffness with glycation.

Our biochemical data show a significant increase in both fluorescence and pentosidine content in glycated samples as compared to the untreated tissue (Fig. 6) ( $p < 0.0001$  for fluorescence and  $p = 0.0007$  for pentosidine). On the other hand, there was no significant difference between glycated and sham-incubated samples with respect to pentosidine or fluorescence.

The best-fit values for the coefficients of our previously proposed strain energy function (Eq. (1)) were  $\{0.113, 0.00379, 0.00173, 39.3, 0.0248, 3.143, 0.0926, 1.91, 57.6^\circ\}$  and the sum of the error squared for this model was 1.91. For the modified strain energy function (Eq. (2)), the coefficients were  $\{0.0876, 0.00415, 0.00378, 32.2, 0.0237, 0.00190, 0.000226, 7.48, 0.0456, 0.000408, 1.75, 56.8^\circ\}$  and the sum of the error squared was 1.37, a 28% improvement in the goodness-of-fit over our previously proposed model. The coefficient  $a'_4$  was 93% greater than  $a_4$ , while  $a'_5$  was 81% greater than  $a_5$ . The coefficients of this modified model resulted in stress–stretch curves that lie within

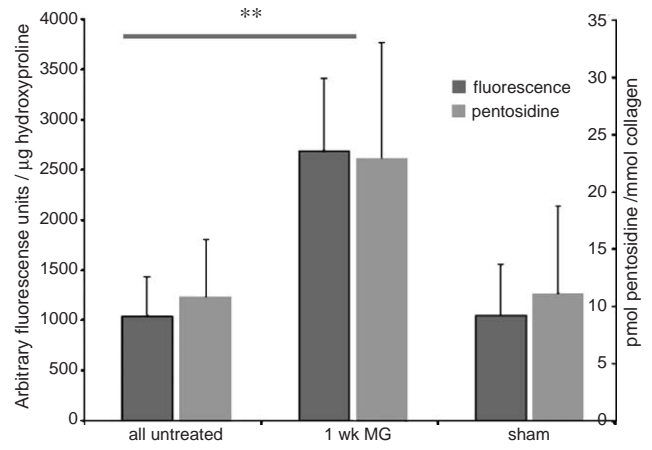


Fig. 6. Biochemical data demonstrate a significant increase in both fluorescence at excitation/emission wavelengths of 370/440 nm and pentosidine content with the 1-week incubation in methylglyoxal (MG) as compared to the untreated tissue, indicating an increase in nonenzymatic crosslink density. No such increase is seen with the 1-week sham incubation. \*\* indicates  $p < 0.025$ .

one standard deviation of the experimental deformations (Fig. 7). Although we were able to find other solutions to the nonlinear regression by choosing different starting values, all other solutions led to strain energy functions that were not positive definite as the laws of thermodynamic require. The largest value of the covariance matrix was 0.65 for the coefficients  $b_4$  and  $b_5$ . Besides the two interactions terms, the values of the covariance matrix were all below 0.5.

#### 4. Discussion

Our results demonstrate that glycation stiffens the annular mechanical behavior and may cause a decrease in the Poisson's ratio  $\nu_{32}$ . Further, we show that the interactions terms of our strain energy functions capture the mechanical influence of glycation on the annulus. Specifically, we note that the changes in axial tensile behavior due to increased levels of AGEs can be

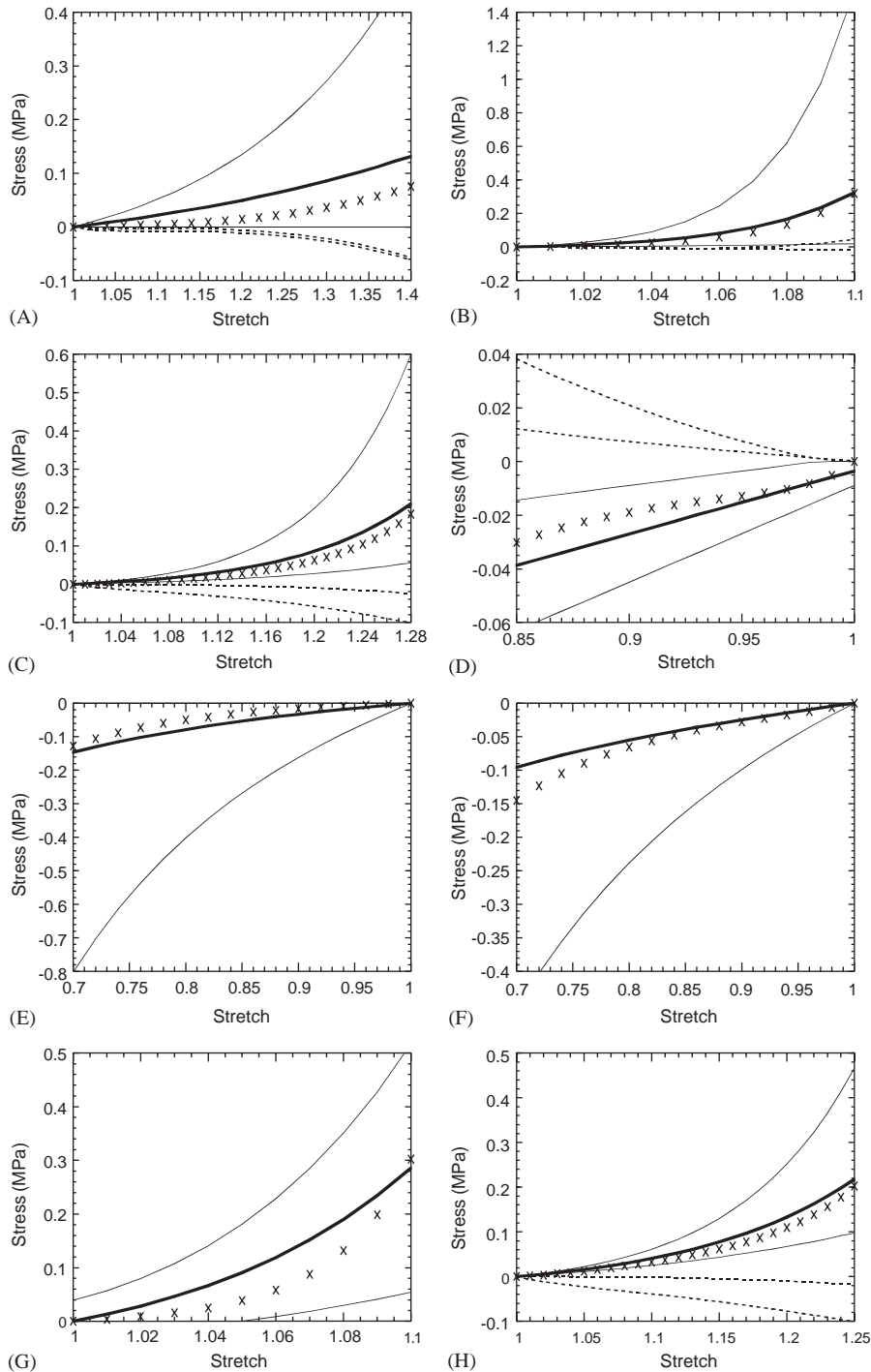


Fig. 7. Results of the simultaneous curve-fit to the measured stress–stretch data and the additional equations representing the stress response for the case of the two traction-free boundary conditions for each experiment A–D and H. A = radial tension (Fujita et al., 1997); B = circumferential tension (Wagner and Lotz, 2004); C = axial tension, before incubation in glycation solution, current study; D = unconfined circumferential compression (Wagner and Lotz, 2004). E = radial confined compression (Klisch and Lotz, 2000); F = axial confined compression (Klisch and Lotz, 2000); G = biaxial tension in the axial direction, circumferential stretch = 1.0 (Bass et al., 2004); H = axial tension, after incubation in glycation solution, adjusted, current study. Solid curves = mean experimental response  $\pm 1$  standard deviation; x = theoretical fit to measured stress–stretch response; dashed lines = theoretical description of stress response for the case of traction-free stress–stretch response for experiments A–D, H.

modeled by increasing only the material coefficients  $a_4$  and  $a_5$  of the interactions terms of our strain energy function in Eq. (2). To our knowledge, this is the first

time that specific material coefficients of a constitutive relationship have been shown to correlate positively with AGE concentrations or with any biochemical

measure. Of course, additional work, such as applying more experimental deformations to glycated tissue, will be required to fully validate the interactions terms.

The accurate representation of the material behavior of the annulus requires that we add a fifth term to our previous strain energy function. This term represents the ability of the crosslinks to resist loading in the direction perpendicular to the collagen fibers. When the annulus is modeled without this term, the sum of the error squared is substantially higher. This is primarily due to the stress response of the traction-free circumferential face in axial experiments (C) and (H), which is substantially worse when the 5th term is not included (data not shown). In a study that was not reported, we held the interactions coefficients  $a_4$  and  $a_5$  constant and attempted to model the change in mechanical behavior with the other material coefficients of the strain energy function in Eq. (2). However, the solution that was generated in this analysis was not positive-definite, suggesting that only the interactions terms represent the mechanical response of the AGEs in a physically relevant way.

We analyzed the covariance matrix of the strain energy function in Eq. (2), as high correlations between the coefficients can suggest that a model is over-parameterized. We found only a moderate correlation between the coefficients of the two interactions terms, and low correlations between coefficients of all other terms. The generally low covariance may be due to the fact that our strain energy function is structurally guided and each term has been designed to represent a specific mechanical response of the tissue's individual structural components.

The pentosidine concentration in the untreated tissue was consistent with that seen by Pokharna and Phillips (1998) in the intervertebral discs of 20–40 year olds, while the concentration after incubation was comparable to that of 40–50 year olds. Although differences in pentosidine concentration with degrees of degeneration have been reported (Duance et al., 1998; Pokharna and Phillips, 1998), the link between pentosidine concentration and degeneration is not as consistent as the link between pentosidine concentration and aging. Efforts to correlate pentosidine concentration and disc degeneration are confounded by the fact that both pentosidine concentration and degeneration increase with age. Given these considerations, we are unable to suggest that the mechanical response of the glycated test specimen is indicative of degenerated tissue.

The sham protocol softens the annular tensile mechanical properties in the axial direction, with no change in the Poisson's ratio. The cause of the softening is currently unknown. The results of a DMMB assay (Farndale et al., 1982) determined that proteoglycans had not diffused from the glycated or control specimens. Furthermore, we measured the size of the grid of ink dots that are used for strain measurement both before

and after the incubation protocol, and found no significant change ( $p > 0.4$  for test specimens,  $p > 0.1$  for sham specimens), indicating that the tissue had not been significantly damaged or degraded.

Although the stress–strain results of the untreated test specimens are softer than those that have been previously reported (Duncan and Lotz, 1998), the data are within one standard deviation of one another. The difference in stiffness between the two studies is likely due to the fact that the test specimens were prepared differently. In the study by Duncan and Lotz, the adjacent vertebral bone was left attached to the annular test specimens, resulting in additional boundary constraints that have a stiffening effect. The mean Poisson's ratio of the untreated test specimen reported in the current study is larger than and just outside of one standard deviation that has been previously reported by others (Elliott and Setton, 2001). On the other hand, the mean Poisson's ratio of the test specimens after incubation in the glycation solution is well within one standard deviation of the previously reported data. Our data indicate a trend of decreasing Poisson's ratio with increasing AGE density. If this trend is real, then it may explain the Poisson's ratio discrepancy between our data and those of Elliott and Setton. The donors in the current study were significantly younger than those in the previous study, therefore our untreated test specimens would likely have had a smaller AGE density, which may have resulted in the higher measured Poisson's ratio.

The strain energy function that is presented here is a structurally guided constitutive relationship, with material properties that are defined by specific features of annular tissue architecture. This constitutive model is a first step towards understanding the interrelationship between specific macromolecular features of the tissue and its mechanical function. In the future, this structurally guided approach may be a significant advance beyond existing phenomenological constitutive models, as it can be used to explore the structure–function relationships of the annulus and the pathomechanics of aging and degeneration in the intervertebral disc.

## Acknowledgments

This research was sponsored by funding from the National Institutes of Health (AR44179).

## References

- Acaroglu, E.R., Iatridis, J.C., Setton, L.A., Foster, R.J., Mow, V.C., Weidenbaum, M., 1995. Degeneration and aging affect the tensile behavior of human lumbar annulus fibrosus. *Spine* 20 (24), 2690–2701.

- Anderson, S.S., Kim, Y., Tsilibary, E.C., 1994. Effects of matrix glycation on mesangial cell adhesion, spreading and proliferation. *Kidney International* 46 (5), 1359–1367.
- Bass, E.C., Ashford, F.A., Segal, M.R., Lotz, J.C., 2004. Biaxial testing of human annulus fibrosus and its implications for a constitutive formulation. *Annals of Biomedical Engineering* 32 (9), 1231–1242.
- Cassidy, J.J., Hiltner, A., Baer, E., 1989. Hierarchical structure of the intervertebral disc. *Connective Tissue Research* 23 (1), 75–88.
- Chen, A.C., Temple, M.M., Ng, D.M., Verzijl, N., DeGroot, J., TeKoppele, J.M., Sah, R.L., 2002. Induction of advanced glycation end products and alterations of the tensile properties of articular cartilage. *Arthritis and Rheumatism* 46 (12), 3212–3217.
- Duance, V.C., Crean, J.K., Sims, T.J., Avery, N., Smith, S., Menage, J., Eisenstein, S.M., Roberts, S., 1998. Changes in collagen cross-linking in degenerative disc disease and scoliosis. *Spine* 23 (23), 2545–2551.
- Duncan, N.A., Lotz, J.C., 1998. Experimental validation of a porohyperelastic finite element model of the annulus fibrosus. In: Middleton, J., Jones, M.L., Pande, G.N. (Eds.), *Computer Methods in Biomechanics & Biomedical Engineering*. Gordon and Breach, London.
- Elliott, D.M., Setton, L.A., 2001. Anisotropic and inhomogeneous tensile behavior of the human annulus fibrosus: experimental measurement and material model predictions. *Journal of Biomechanical Engineering* 123, 256–263.
- Farndale, R.W., Sayers, C.A., Barrett, A.J., 1982. A direct spectrophotometric microassay for sulfated glycosaminoglycans in cartilage cultures. *Connective Tissue Research* 9 (4), 247–248.
- Fujita, Y., Duncan, N.A., Lotz, J.C., 1997. Radial tensile properties of the lumbar annulus fibrosus are site and degeneration dependent. *Journal of Orthopaedic Research* 15 (6), 814–819.
- Fung, Y.C.B., 1967. Elasticity of soft tissues in simple elongation. *American Journal of Physiology* 213 (6), 1532–1544.
- Hormel, S.E., Eyre, D.R., 1991. Collagen in the ageing human intervertebral disc: an increase in covalently bound fluorophores and chromophores. *Biochimica et Biophysica Acta* 1078 (2), 243–250.
- Hukins, D.W.L., 1988. Disc structure and function. In: Ghosh, P. (Ed.), *The Biology of the Intervertebral Disc*. CRC Press, Boca Raton FL, pp. 1–39.
- Iatridis, J.C., Setton, L.A., Foster, R.J., Rawlins, B.A., Weidenbaum, M., Mow, V.C., 1998. Degeneration affects the anisotropic and nonlinear behaviors of human annulus fibrosus in compression. *Journal of Biomechanics* 31 (6), 535–544.
- Kenedi, R.M., Gibson, T., Daly, C.H., 1965. Bio-engineering studies of the human skin. The effects of unidirectional tension. In: Jackson, S.F., Harkness, R.D., Partridge, S.M., Tristman, G.R. (Eds.), *Structure and Function of Connective and Skeletal Tissue*. Butterworths, London.
- Klisch, S.M., Lotz, J.C., 1999. Application of a fiber reinforced continuum theory to multiple deformations of the annulus fibrosus. *Journal of Biomechanics* 32, 1027–1036.
- Klisch, S.M., Lotz, J.C., 2000. A special theory of biphasic mixtures and experimental results for human annulus fibrosus tested in confined compression. *Journal of Biomechanical Engineering* 122, 180–188.
- Marchand, F., Ahmed, A.M., 1990. Investigation of the laminate structure of lumbar disc annulus fibrosus. *Spine* 15 (5), 402–410.
- Monnier, V.M., Kohn, R.R., Cerami, A., 1984. Accelerated age-related browning of human collagen in diabetes mellitus. *Proceedings of the National Academy of Sciences of United States of America* 81 (2), 583–587.
- Pokharna, H.K., Phillips, F.M., 1998. Collagen crosslinks in human lumbar intervertebral disc aging [see comments]. *Spine* 23 (15), 1645–1648.
- Reihnsner, R., Menzel, E.J., 1998. Two-dimensional stress-relaxation behavior of human skin as influenced by non-enzymatic glycation and the inhibitory agent aminoguanidine. *Journal of Biomechanics* 31, 985–993.
- Reiser, K.M., 1994. Influence of age and long-term dietary restriction on enzymatically mediated crosslinks and nonenzymatic glycation of collagen in mice. *Journal of Gerontology* 49 (2), B71–B79.
- Reiser, K.M., 1998. Nonenzymatic glycation in aging and diabetes. *Proceedings of the Society for Experimental Biology and Medicine* 218, 23–37.
- Sell, D.R., Monnier, V.M., 1989. Structure elucidation of a senescence cross-link from extracellular matrix. *Journal of Biological Chemistry* 264, 21597–21602.
- Spencer, A.J.M., 1984. *Continuum Theory of the Mechanics of Fibre-Reinforced Composites*. Springer, New York.
- Thompson, J.P., Pearce, R.H., Schechter, M.T., Adams, M.E., Tsang, I.K.Y., Bishop, P.B., 1990. Preliminary evaluation of a scheme for grading the gross morphology of the human intervertebral disc. *Spine* 15 (5), 411–415.
- Thorpe, S.R., Baynes, J.W., 2003. Maillard reaction products in tissue proteins: new products and new perspectives. *Amino Acids* 25 (3–4), 275–281.
- Verzijl, N., DeGroot, J., Zaken, C.B., Braun-Benjamin, O., Maroudas, A., Bank, R.A., Mizrahi, J., Schalkwijk, C.G., Thorpe, S.R., Baynes, J.W., Bijlsma, J.W.J., Lefeber, F.P.J.G., TeKoppele, J.M., 2002. Crosslinking by advanced glycation end product increases the stiffness of the collagen network in human articular cartilage: a possible mechanism through which age is a risk factor for osteoarthritis. *Arthritis and Rheumatism* 46 (1), 114–123.
- Wagner, D.R., Lotz, J.C., 2004. Theoretical model and experimental results for the a nonlinear strain energy function for the elastic behavior of human annulus fibrosus. *Journal of Orthopaedic Research* 22 (4), 901–909.
- Woessner, J.F., 1961. The determination of hydroxyproline in tissue and protein samples containing small proportions of this amino acid. *Archives of Biochemistry and Biophysics* 93, 440–447.
- Wolffebuttel, B.H., Boulanger, C.M., Crijs, F.R., Huijberts, M.S., Poitevin, P., Swennen, G.N., Vasan, S., Egan, J.J., Ulrich, P., Cerami, A., Levy, B.I., 1998. Breakers of advanced glycation end products restore large artery properties in experimental diabetes. *Proceedings of the National Academy of Sciences of United States of America* 95 (8), 4630–4634.